*Int. J. Electrochem. Sci.*, 15 **(2020)** 6930 – 6937, doi: 10.20964/2020.07.73

International Journal of
ELECTROCHEMICAL
SCIENCE
www.electrochemsci.org

*Short Communication*

# Facile Preparation of $Cu^{2+}$-doped Tin(IV) Pyrophosphate /Potassium Metaphosphate Composite as a Highly Efficient Electrolyte for Intermediate Temperature SOFCs

*RuijuanShi, Jingjing Zhu, Peng Sun, Nan Wang, Junlong Liu*[*], *Hongtao Wang*[*]

School of Chemical and Material Engineering, Fuyang Normal University; Anhui Provincial Key Laboratory for Degradation and Monitoring of Pollution of the Environment, Fuyang 236037, China
[*]E-mail: hwang@fynu.edu.cn, jlliu@fynu.edu.cn

*Received:* 3 March 2020 / *Accepted:* 29 April 2020 / *Published:* 10 June 2020

In this study, a $Sn_{0.95}Cu_{0.05}P_2O_7/KPO_3$ composite ceramic was synthesized via a facile solid state reaction method and characterized by X-ray diffractometer (XRD), scanning electron microscopy (SEM) and Raman spectroscopy. The intermediate temperature electrical properties were evaluated using impedance spectroscopy. The results showed that the microstructure of the $Sn_{0.95}Cu_{0.05}P_2O_7/KPO_3$ electrolyte pellet plays an important role in determining electrical properties, and amorphous secondary phases appreciably influence proton conduction. The highest conductivity of $Sn_{0.95}Cu_{0.05}P_2O_7/KPO_3$ was $3.4\times10^{-2}$ $S\cdot cm^{-1}$ in a dry nitrogen atmosphere at 700 °C. The operation tests of an $H_2/O_2$ fuel cell with the $Sn_{0.95}Cu_{0.05}P_2O_7/KPO_3$ composite electrolyte showed an open circuit voltage of approximately 1.06 V and a maximum power output density of 218.9 $mW\cdot cm^{-2}$ at 700 °C. This work offers new alternatives for the design of metal pyrophosphates composite electrolyte.

**Keywords:** Pyrophosphates; Composite electrolyte; Ionic conductivity; Solid oxide fuel cell

## 1. INTRODUCTION

Fuel cells are a promising technology for the efficient and environmentally friendly generation of electrical power [1-6]. Proton-conducting electrolyte materials at intermediate temperatures are in high demand for fuel cells, because they are more convenient for the practical application of intermediate temperature solid oxide fuel cells (IT-SOFCs), as they have no problems in terms of fuel recycling and dilution compared with oxygen ion electrolyte materials [7-13].

Metal pyrophosphates $MP_2O_7$ (M = $Sn^{4+}$, $Ge^{4+}$, $Si^{4+}$, $Zr^{4+}$, $Ce^{4+}$, and $Ti^{4+}$ etc.) are of great interest for IT-SOFCs due to their high proton conductivities [14-15]. Among the pyrophosphates, tin(IV) pyrophosphate ($SnP_2O_7$) has been intensively investigated owing to its high proton conductivity. Especially, through partial substitution of $Sn^{4+}$ with other metal cations such as $Zn^{2+}$, $Mn^{2+}$, $Mg^{2+}$, $Al^{3+}$,

$In^{3+}$, $Sb^{3+}$, $Ce^{4+}$, $Sb^{5+}$ and $Mo^{6+}$, $SnP_2O_7$ composites display enhanced proton conductivities [16-27]. Nevertheless, it is difficult to fabricate dense electrolytes which limits their widespread application in IT-SOFCs. High temperature (>1400 °C) is required for a complete densification of pyrophosphates, and this leads to a series of problems, such as the evaporation of excess phosphate phase and the decrease of conductivity [16, 21, 25]. Tao et al. studied the synthesis and characterization of doped tin(IV) pyrophosphates $Sn_{0.92}In_{0.08}(P_2O_7)_{1-\delta}$ and $Sn_{0.9}Sc_{0.1}(P_2O_7)_{1-\delta}$, and found that the high proton conductivity under anhydrous conditions depended on the synthetic history, and amorphous phosphorous rich phase along the grain boundaries facilitates good conductivity [26-27]. Similar results were reported by Anfimova et al. [14]. In order to synthesize metal pyrophosphates with high ionic conductivity and stability under lower temperatures, we have fabricated dense pyrophosphate-containing composites $Sn_{0.95}Al_{0.05}P_2O_7/KSn_2(PO_4)_3$ and $Sn_{0.9}Mg_{0.1}P_2O_7/KSn_2(PO_4)_3$ and both showed improved electrical performance compared with pure pyrophosphates [28-29].

In this paper, a $SnP_2O_7/KPO_3$ composite with a partial substitution of Sn by Cu was synthesized using a facile solid state reaction method, in which carbonate salt $K_2CO_3$ was also employed for doping. The composite was characterized by XRD, Raman and SEM. The intermediate temperature electrical properties were determined by using impedance spectroscopy, and an $H_2/O_2$ fuel cell using the $Sn_{0.95}Cu_{0.05}P_2O_7/KPO_3$ composite as electrolyte membrane was constructed.

## 2. EXPERIMENTAL

The $Sn_{0.95}Cu_{0.05}P_2O_7/KPO_3$ composite was synthesized via a solid state reaction method. Stoichiometric ratio of $Cu(NO_3)_2$ and $SnO_2$ were mixed thoroughly with $H_3PO_4$, and then the milled mixture was dried in an oven. Subsequently, $K_2CO_3$ was added to the mixed powder. After grinding, the gray-white product was heated at 550 ℃ for 2 h in a covered alumina crucible. The resulting solid composite particles were ground and sieved and pressed at 15 MPa, and re-sintered at 720 °C for 1 h to obtain the $Sn_{0.95}Cu_{0.05}P_2O_7/KPO_3$ electrolyte disc (1.0 mm in thickness).

The phase determination of the $Sn_{0.95}Cu_{0.05}P_2O_7/KPO_3$ powder was characterized by X–ray powder diffraction (XRD) using a X' Pert-pro MPD diffractometer using Cu Kα radiation (λ = 1.5432 Å) over 2θ range from 15 to 70°. The microstructural analysis of the $Sn_{0.95}Cu_{0.05}P_2O_7/KPO_3$ pellet by scanning electron microscopy (SEM) was carried out on a FEI Tecnai G2 F30 electron microscope. The Raman spectrum was obtained by invia spectrometer (Renishaw, Gloucestershire, United Kingdom).

For the conductivity measurements and fuel cell tests, the sintered $Sn_{0.95}Cu_{0.05}P_2O_7/KPO_3$ pellet was polished with sandpaper, painted with 20 %Pd-80 %Ag paste on both sides, dried in an oven and then, two Ag wires were separately connected to each side of the painted pellet to be used as current collectors. The electrochemical impedance spectroscopy (EIS) was measured at the frequency ranging from 1 Hz to $10^6$ Hz with an AC amplitude of 20 mV using a CHI-660E electrochemical setup.

## 3. RESULTS AND DISCUSSION

The XRD pattern of the $Sn_{0.95}Cu_{0.05}P_2O_7/KPO_3$ composite powder is shown in Fig. 1. It can be seen that almost all of the diffraction peaks could be assigned to the cubic $SnP_2O_7$ phase. However, small characteristic peaks of $SnO_2$ appeared at the diffraction angle 2θ = 26.82°, suggesting that secondary

$SnO_2$ phase formed in the bulk of the composite particles, which can be considered to be the result of the reaction of $SnP_2O_7 + K_2CO_3 = SnO_2 + 2KPO_3 + CO_2\uparrow$. No $K_2CO_3$, and $KPO_3$ diffraction peaks were observed in the XRD due to their weak crystallization or/and good dispersion. These amorphous phases around the grain boundary may facilitate the good proton conductivity [14, 17, 26-27].

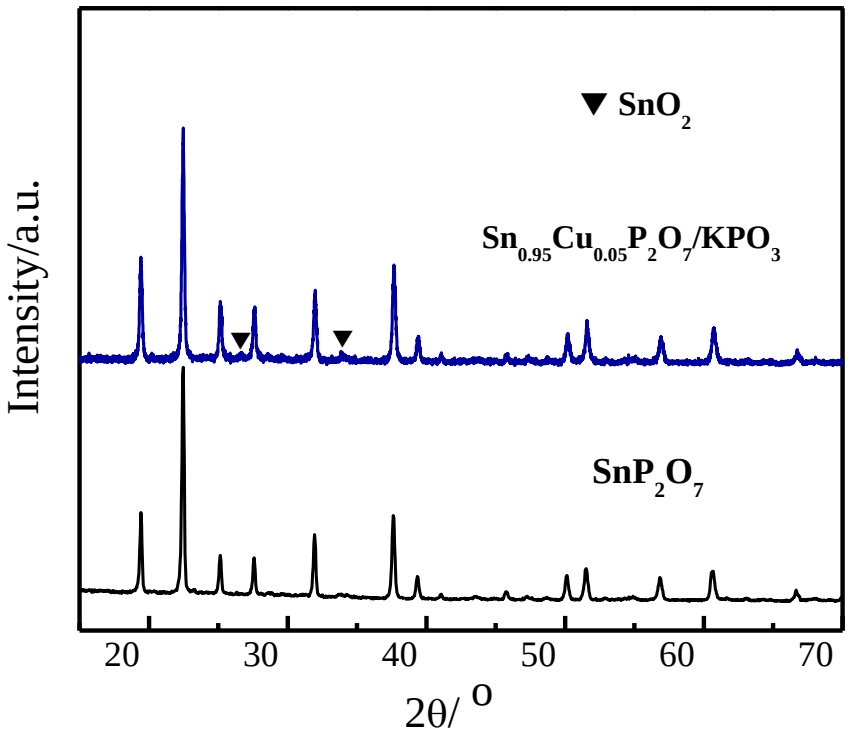


**Figure 1.** XRD pattern of the $Sn_{0.95}Cu_{0.05}P_2O_7/KPO_3$ composite.

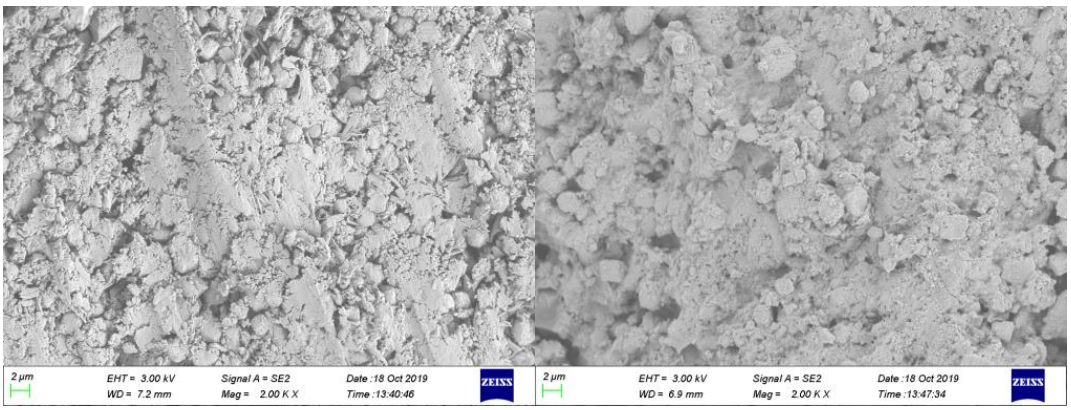


**Figure 2.** SEM surface (a) and cross-sectional (b) images of the $Sn_{0.95}Cu_{0.05}P_2O_7/KPO_3$ pellet.

The microstructure of the $Sn_{0.95}Cu_{0.05}P_2O_7/KPO_3$ pellet is shown in Fig.2. It was observed from the SEM images that a non-porous, crack-free and dense electrolyte pellet was produced by sintering at 720 °C, which suggests that the transportation of ions might be convenient and the crossover of $O_2$ or fuel gas through the composite pellet might be negligible. Meanwhile, the powders are much finer than

that of $M^{n+}$-doped $SnP_2O_7$ synthesized by the conventional solid state method using metal oxide substrate and phosphoric acid, which means the presence of inorganic carbonate on the precursors plays a significant role in the formation of homogeneous, fine particles [28-29]. It can be expected that the microstructure of the electrolyte pellet and the fine amorphous secondary phase surrounding the grain boundaries would appreciably influence the proton conduction [14, 26].

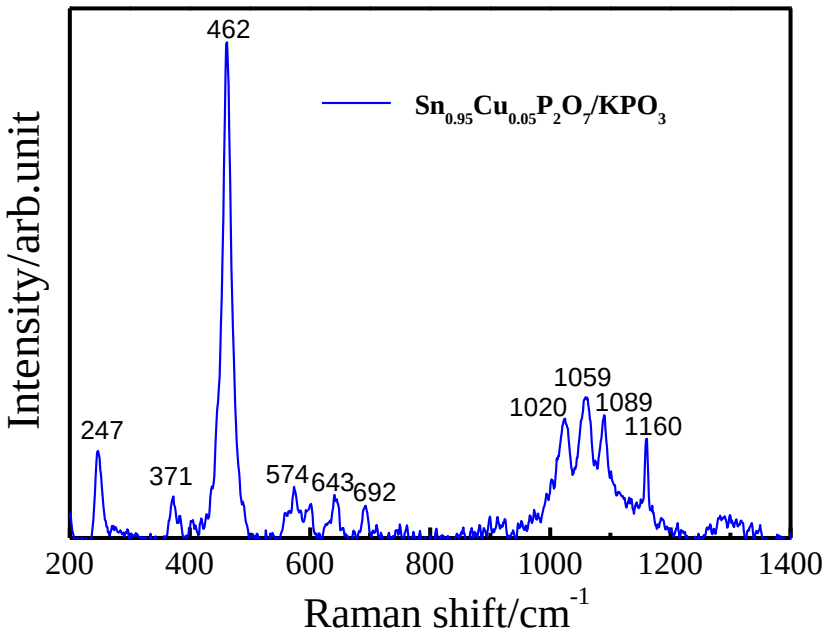


**Figure 3.** Raman spectrum of the $Sn_{0.95}Cu_{0.05}P_2O_7/KPO_3$ composite.

The Raman spectrum of the $Sn_{0.95}Cu_{0.05}P_2O_7/KPO_3$ composite is presented in Fig.3. The bands in the low frequency between 200 and 400 $cm^{-1}$ are assigned to the bending vibrations of the $PO_4$ tetrahedron in pyrophosphate and the band at 462 $cm^{-1}$ is attributed to the vibration of the Cu-O-P and Sn-O-P chains. The bands at 643-692 $cm^{-1}$ are assigned to the symmetric stretching vibrations of the P-O-P bonds in metaphosphate, while the band at 1059 $cm^{-1}$ is attributed to the symmetric stretching vibrations of the P-O-P in pyrophosphate. The band at 1160 $cm^{-1}$ is attributed to the symmetric stretching vibrations of the $PO_2^-$ in metaphosphate [30]. The Raman spectrum revealed the presence of metal pyrophosphate and metaphosphate in the prepared composite in this study.

The log ($\sigma$T) ~ 1000 $T^{-1}$ plots of the $Sn_{0.95}Cu_{0.05}P_2O_7/KPO_3$ composite were measured in the temperature range of 450 °C ~ 700 °C under a dry nitrogen atmosphere, as shown in Fig.4, and compared with the conductivity performance of previously reported $Sn_{0.9}In_{0.1}P_2O_7$ [25] electrolyte materials. The conductivity of the $Sn_{0.95}Cu_{0.05}P_2O_7/KPO_3$ composite decreased from $3.4\times10^{-2}$ $S\cdot cm^{-1}$ to $3.1\times10^{-5}$ $S\cdot cm^{-1}$ from 700 °C to 450 °C. The conductivities of $Sn_{0.92}In_{0.08}(P_2O_7)_{1-\delta}$ prepared by an aqueous solution method reported by Tao [26] are $6.5\times10^{-6}$ $S\cdot cm^{-1}$ and $8.0\times10^{-9}$ $S\cdot cm^{-1}$ at 900 and 400 °C in air, respectively. The highest conductivity is $1.15\times10^{-6}$ $S\cdot cm^{-1}$ for $Ce_{0.88}Mn_{0.12}P_2O_7$ at 450 °C and $2.15\times10^{-5}$ $S\cdot cm^{-1}$ for $Sn_{0.88}Mn_{0.12}P_2O_7$ at 750° C (reported by Singh et al. [31]). It can be seen that the proton conductivities of the $Sn_{0.95}Cu_{0.05}P_2O_7/KPO_3$ composite are higher than that of $Sn_{0.92}In_{0.08}(P_2O_7)_{1-\delta}$ and

$Sn_{0.88}Mn_{0.12}P_2O_7$. When the sintered temperature is above 600 °C, the conductivities of $Sn_{0.9}In_{0.1}P_2O_7$ calcined at 650 °C are lower than that of the $Sn_{0.95}Cu_{0.05}P_2O_7/KPO_3$ composite. It is suggested that sintering at elevated temperature leads to the evaporation of phosphate phase, which results in reduced proton transport pathways and lowered proton conductivity [25]. The result suggests that the conductivity related to the preparation method, calcination temperature and the existence of fine amorphous phase, which was evident by SEM microscopy may be responsible for the difference in proton conductivity [14, 17, 26].

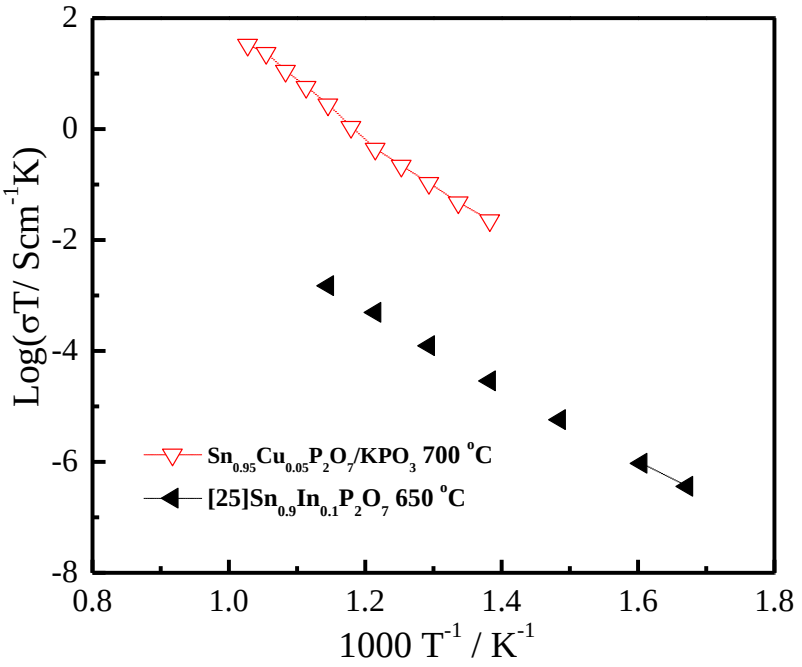


**Figure 4.** The log (σT) ~ 1000 $T^{-1}$ plots of the $Sn_{0.95}Cu_{0.05}P_2O_7/KPO_3$ composite.

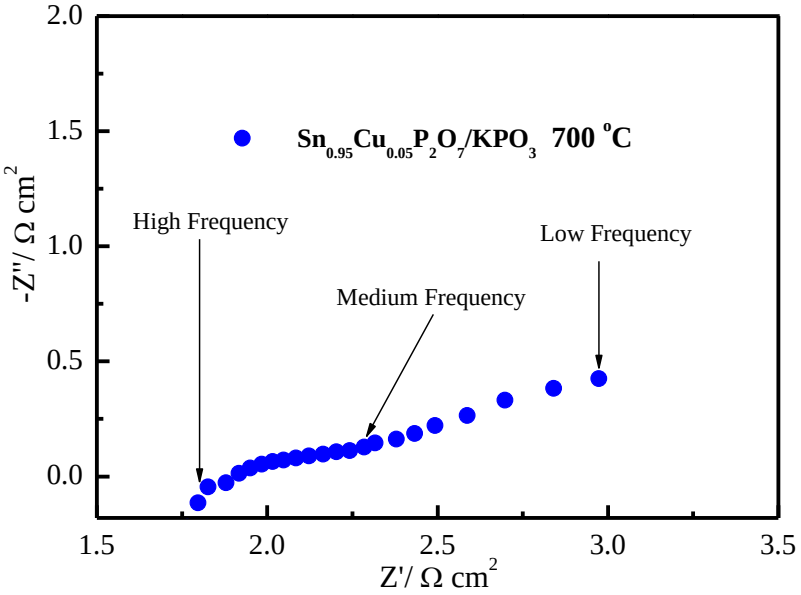


**Figure 5.** Electrochemical impedance spectrum of the $Sn_{0.95}Cu_{0.05}P_2O_7/KPO_3$ composite.

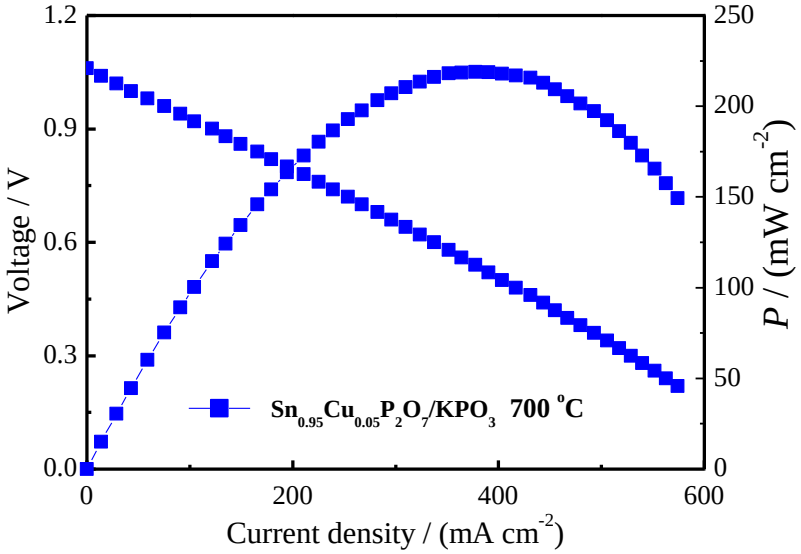


**Figure 6.** *I-V-P* curves of the $H_2/O_2$ fuel cell with the $Sn_{0.95}Cu_{0.05}P_2O_7/KPO_3$ as electrolyte at 700 °C.

Fig. 5 shows the electrochemical impedance spectrum of the $Sn_{0.95}Cu_{0.05}P_2O_7/KPO_3$ composite under an open circuit condition at 700 °. A semicircle in the high frequency region and an arc in the low frequency region in the Nyquist plot can be seen. The semicircle in the high frequency region may correspond to the grain boundary resistances, and the arc in the low frequency region may correspond to the bulk resistances [25]. And the arc is superposed on the semicircle in the low frequency region, which demonstrates that the $Sn_{0.95}Cu_{0.05}P_2O_7/KPO_3$ composite has good conductivity.

The $H_2/O_2$ fuel cell performance was tested with the $Sn_{0.95}Cu_{0.05}P_2O_7/KPO_3$ composite as electrolyte at 700 °C. The *I-V-P* curves of the $H_2/O_2$ fuel cell are shown in Fig. 6. An open circuit voltage of approximately 1.06 V was obtained, which demonstrates that the $Sn_{0.95}Cu_{0.05}P_2O_7/KPO_3$ composite electrolyte is a fully dense layer and the gas leakage through the electrolyte is negligible. The power output density reached a maximum value of 218.9 $mW \cdot cm^{-2}$ at 700 °C, which is higher than most of the previously reported fuel cells using $SnP_2O_7$-based electrolyte materials. We have reported that the power output density of dense pyrophosphate-containing composites $Sn_{0.95}Al_{0.05}P_2O_7/KSn_2(PO_4)_3$ and $Sn_{0.9}Mg_{0.1}P_2O_7/KSn_2(PO_4)_3$ were only 142.1 $mW \cdot cm^{-2}$ and 130.9 $mW \cdot cm^{-2}$ at 700 °C, respectively [28-29]. These results demonstrate that the $Sn_{0.95}Cu_{0.05}P_2O_7/KPO_3$ composite is a new alternative electrolyte for IT-SOFCs.

## 4. CONCLUSIONS

A new $Sn_{0.95}Cu_{0.05}P_2O_7/KPO_3$ composite electrolyte was prepared by solid state reaction method, and structure, electrical properties and ionic conduction were characterized. The results showed that almost all of the diffraction peaks were assigned to the cubic $SnP_2O_7$ phase and dense $Sn_{0.95}Cu_{0.05}P_2O_7/KPO_3$ electrolyte was obtained by sintering at 720 °C. The microstructure of the electrolyte pellet plays an important role in determining electrical properties and amorphous secondary

phases appreciably influence the proton conduction. The highest conductivity obtained for $Sn_{0.95}Cu_{0.05}P_2O_7/KPO_3$ composite was $3.4\times10^{-2}$ $S\cdot cm^{-1}$ at 700 °C. The $H_2/O_2$ fuel cell showed a maximum power output density of 218.9 $mW\cdot cm^{-2}$ at 700 °C. The results of this work offer new alternatives for the design of metal pyrophosphates composite electrolyte which has the potential to meet the requirements for application in IT-SOFCs.

ACKNOWLEDGEMENTS
This work was supported by the Natural Science Project of Anhui Province Department of Education (No. KJ2019A0539), Horizontal cooperation project of Fuyang municipal government and Fuyang Normal College (No. XDHXTD201704, XDHX201739), Excellent Youth Foundation of Fuyang Normal College (rcxm201805) and Foundation of Anhui Provincial Key Laboratory for Degradation and Monitoring of Pollution of the Environment (2019HJJC01ZD).

## References

1. L. Bi, S.P. Shafi, E.H. Da'as and E. Traversa, *Small*, 14 (2018) 1801231.
2. C. Bernuy-Lopez, L. Rioja-Monllor, T. Nakamura, S. Ricote, R. O'Hayre, K. Amezawa, M. Einarsrud and T. Grande, *Materials*, 11 (2018) 196.
3. Y.P. Xia, Z.Z. Jin, H.Q. Wang, Z. Gong, H.L. Lv, R.R. Peng, W. Liu and L. Bi, *J. Mater. Chem. A*, 7 (2019) 16136.
4. Y. Tian, Z. Lü, X. Guo and P. Wu, *Int. J. Electrochem. Sci*., 14 (2019) 1093.
5. X. Xu, L. Bi and X.S. Zhao, *J. Membrane Sci.*, 558 (2018) 17.
6. A.A. Solovyev, S.V. Rabotkin, A.V. Shipilova and I.V. Ionov, *Int. J. Electrochem. Sci*., 14 (2019) 575.
7. X. Xu, H.Q. Wang, J.M. Ma, W.Y. Liu, X.F. Wang, M. Fronzi and L. Bi, *J. Mater. Chem. A*, 7 (2019) 18792.
8. H. Jiang and F. Zhang, *Int. J. Electrochem. Sci*., 15 (2020) 959.
9. J.M. Ma, Z.T. Tao, H.N. Kou, M. Fronzi and L. Bi, *Ceram. Int.*, 46 (2020) 4000.
10. H. Dai, H. Kou, Z. Tao, K. Liu, M. Xue, Q. Zhang, L. Bi, *Ceram. Int.*, 46 (2020) 6987.
11. E. H. Da´as, L. Bi, S. Boulfrad and E. Traversa, *Sci. China Mater*., 61 (2018) 57.
12. J.-W. Ju, D.-M. Huan, Y.-X. Zhang, C.-R. Xia, G.-L. Cui, *Rare Met.*, 37 (2018) 734.
13. Y. N. Chen, T. Tian, Z. H. Wan, F. Wu, J. T. Tan and M. Pan, *Int. J. Electrochem. Sci.*, 13 (2018) 3827.
14. T. Anfimova, T. Lie-Andersen, E.P. Jensen, C.B. Prag, U.G. Nielsen, D.R. Sørensen, E.M. Skou, E. Christensen, N.J. Bjerrum and Q. Li, *Solid State Ionics*, 278 (2015) 209.
15. B. Singh, H-N. Im, J-Y. Park and S-J. Song, *J. Phys. Chem. C,* 117 (2013) 2653.
16. V. Nalini, R. Haugsrud and T. Norby, *Solid State Ionics*, 181 (2010) 510.
17. M. Nagao, T. Kamiya, P. Heo, A. Tomita, T. Hibino and M. Sano, *J. Electrochem. Soc.*, 153 (2006) A1604.
18. J. Xiao, H.M. Zhang, Z.J. Yang, H.T. Wang, G.L. Ma and Z.F. Zhou, *J. Alloys Compd.*, 521 (2012) 106.
19. B. Singh, J. Kim, J. Park and S. Song, *J. Eur. Ceram. Soc.*, 34 (2014) 2967.
20. K. Genzaki, P. Heo, M. Sano and T. Hibino, *J. Electrochem. Soc.*, 156 (2009) B806.
21. A. Tomita, N. Kajiyama, T. Kamiya, M. Nagao and T. Hibino, *J. Electrochem. Soc.*, 154 (2007) B1265.
22. X. Wu, A. Verma and K. Scott, *Fuel Cells*, 8 (2008) 453.
23. T. Hibino, Y. Shen, M. Nishida and M. Nagao, *Angew. Chem. Int. Ed.*, 51 (2012) 10786.

24. T. Hibino and K. Kobayashi, *J. Mater. Chem. A*, 1 (2013) 6934.
25. S.R. Phadke, C.R. Bowers, E.D. Wachsman and J.C. Nino, *Solid State Ionics*, 183 (2011) 26.
26. S. Tao, Solid State Ionics 180 (2009) 148.
27. R. Lan and S. W. Tao, *J. Alloys Compd.*, 486 (2009) 380.
28. J. Liu, R. Du, R. Shi, H. Wang, *Ceram. Int.*, 44 (2018) 5179.
29. J. Liu, R. Du, R. Shi, H. Wang, *Int. J. Electrochem. Sci*., 13 (2018) 5061.
30. P. A. Bingham and R. J. Hand, Mater. Res. Bull., 43 (2018) 1679.
31. B. Singh, J.H. Kim, O. Parkash and S. Song, *Ceram. Int.*, 42 (2016) 2983.